Evaluation of geometric tolerances using strain energy density

N.B. When citing this work, cite the original published paper.

(article starts on next page)
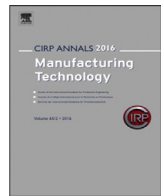
Evaluation of geometric tolerances using strain energy density

Kristina Wärmefjord[a,*], Lars Lindkvist[a], Rikard Söderberg (1)[a], Björn Lindau[b], Maria Andrén[b]

[a] *Chalmers University of Technology, Dept. of Industrial and Materials Science, SE 412-96 Gothenburg, Sweden*
[b] *Volvo Cars, Gothenburg, Sweden*

ARTICLE INFO

ABSTRACT

Traditionally, the geometric quality of assembled products has been evaluated by deviation from nominal values. However, the increased use mixed materials in especially automotive industry, in combination with an increased use of non-rigid simulation, open up for other evaluation criteria to complement the traditionally used deviation. The stiffness of a part or subassembly will, in combination with its deviation from nominal, give rise to different amounts of energy needed to join it to other parts. In this paper, the energy needed for joining is suggested as an evaluation criterion, complementary to geometric deviation, to judge the severity of the deviation.

1. Introduction

Variation in manufacturing processes is unavoidable and tolerancing is a way to specify the allowed variation, aiming to secure product quality [1]. The tolerances are related to cost, and tighter tolerances usually drive a higher cost [2,3]. The tolerance design is often based on digital tools, i.e. Computer Aided Tolerancing (CAT). Using CAT tools, the resulting variation on assembly level can be predicted based on inspection data or tolerances on part level, and a model relating part deviations to assembly deviations [4]. CAT tools have developed over the years and become more advanced. A good CAT tool is characterized by accuracy, reasonable calculation times and its ease of use. It should also provide the ability to include the compliant behavior of non-rigid parts. For rigid parts, different tolerance analysis models can be applied to evaluate the effect of part tolerances on assembly level [5]. Over the years, digital tools have become more and more important in the product development cycle [6], and CAT tools, being an important part in the set of digital tools, are used to make sure that both the producability and the quality of a mechanical product can be fulfilled.

Traditionally, tolerance specification and analysis, usually relying on the assumption of rigid parts, evaluate deviation from nominal and variation around the mean deviation on assembly level. This is also how the requirements on assembly level are set. Usually, also non-rigid variation simulation follows this regime and predicts the distributions of dimensional deviations on assembly level, even if there are examples of evaluation of stress [7], forces [8] and vibrations [9] during the joining process or other performance measures [10]. An entropy-based method to evaluate how the strain-energy distribution affects assembly accuracy for machined parts was suggested by [11].

The standards ASME Y14.5 and ISO 1101 [12,13] consider flexible (i. e. non-rigid) parts, but with a focus on the specification method to communicate the requirements on a part. There are also scientific works on how to inspect non-rigid parts and how to compensate for gravity and other forces affecting the parts during inspection [14−16].

This paper aims at discussing alternatives and complements to the traditional evaluation criterion based on deviation and/or variation, and points out a criterion that might be useful to evaluate the severity of a deviation of a non-rigid part or subassembly.

1.1. Scope of the paper

This paper suggests a new complementary evaluation criterion for non-rigid variation simulation, based on the work or energy required to assemble a part or subassembly to its mating parts. In this way, both the stiffness and the deviation of a part is included in the evaluation. For example, the deviation of a really flexible part or subassembly will be deemed less severe than the same deviation of a very rigid part or subassembly.

In Section 2 an overview of non-rigid variation simulation is given. This is followed by a definition of the suggested evaluation criterion in Section 3. In Section 3, one simple and one industrial case study are used to validate and illustrate the suggested method. A discussion is found in Section 4 and a summary and conclusions are presented in Section 5.

2. Non-rigid variation simulation

A non-rigid Monte Carlo-based variation simulation allows for bending of parts due to part and fixture deviations or other forces affecting the parts. The simulation is based on finite element analysis in combination with the method of influence coefficient (MIC) to save simulation time [17]. In contrast to rigid analysis, where only six locators per part can be allowed, an *N*-2−1 locating scheme can be

allowed, where *N* is an arbitrary number of clamps. The main steps in the simulation are described below. The starting point is two parts, *A* (master part) and *B* (slave part), that are to be joined to the assembly *AB*. The stiffness matrices of the parts are denoted $\mathbf{K}_A$ and $\mathbf{K}_B$, and the part deviations from nominal values in the clamping points are $\mathbf{u}_A$ and $\mathbf{u}_B$.

Step 1. Fixturing/Clamping. The forces needed to close the gaps in the clamping points and to avoid that the two parts penetrate each other are denoted $\mathbf{F}_A$ and $\mathbf{F}_B$.

$$\mathbf{F}_A = \mathbf{K}_A \mathbf{u}_A, \ \ \mathbf{F}_B = \mathbf{K}_B \mathbf{u}_B \tag{1}$$

Step 2. Joining and contact modeling. In this paper, a point-based joining method is assumed, such as spot welding, riveting or screwing. Other joining methods require other modeling techniques [18]. The modeling of the joints is done using contact modeling. For each contact point/node on part *A*, the closest node on part *B* is identified to form a contact pair. The purpose of contact modeling is that the slave part is not allowed to penetrate the master part in any of the contact pairs.

The distance, d_i, between the two nodes in contact pair *i*, is a linear combination of the reaction forces in the slave nodes, R_j. The forces are caused by a collision with the master surface:

$$d_i = \beta_{i0} + R_1 \beta_{i1} + \ldots + R_n \beta_{nm} \tag{2}$$

If $R_i > 0$ in slave node *i*, there must also be resulting forces, F_k, on the master part to maintain the force and moment equilibrium. The resulting forces are distributed over the nodes in the corresponding master element. Moreover, the constraints below should be fulfilled:

3a. $d_i \geq 0, \ \forall i$
3b. $R_i \leq 0, \ \forall i$ (3)
3c. $d_i R_i = 0, \ \forall i$

Constraint *3a* are used to avoid penetrations. Constraint *3b* states that a reaction force must never pull the parts together. Finally, constraint *3c* implies that either $R_i = 0$ or $d_i = 0$, meaning that if the reaction force is negative, it must result in a penetrated distance $d_i = 0$, alternatively if $d_i > 0$ (i.e. no penetration), there can be no reaction force (i.e. $R_i = 0$).

Step 2b. For the joining points, step 2a is redone, but the constraint 3a in Eq. (3) is replaced with $d_i \leq 0$ for all *i*. In this way, the distance $d_i = 0$, for all joining points and the joining nodes are brought together.

The contact problem can be solved iteratively [19] or as a quadratic problem formulation [20,21] to minimize the applied forces.

After applying the forces described above, and with all joining points set, the assembly deviation from nominal is $\boldsymbol{u}_{AB_{clamped}}$ and the assembly has stiffness matrix $\mathbf{K}_{AB}$. For simplicity, all forces required to achieve the shape $\boldsymbol{u}_{AB_{clamped}}$ are summarized in $\mathbf{F}_{AB_{clamped}}$

Step 3. Spring back. Finally, the assembly is released from the overconstrained locating scheme and spring-back occurs. The final deviation of the assembly is denoted **u** and is calculated by applying the forces $\mathbf{F}_{AB_{clamped}}$ from the previous step, but in opposite direction:

$$\boldsymbol{u} = -\boldsymbol{K}_{AB}^{-1} \, \boldsymbol{F}_{AB_{clamped}} \tag{4}$$

The details of the calculations can be found in [22]. The steps above can be included in a Monte Carlo (MC) based variation simulation. In each MC replication the resulting assembly deviation is calculated and by running many MC replications, a distribution of the assembly deviation in each node can be formed. The results are traditionally summarized in a root mean square measure over all nodes or color-coded.

The process briefly described above can be adjusted to different joining methods [18] and other aspects and it can also be used for other purposes than calculating deviation and/or variation, such as calculation of stresses, forces etc.

3. An energy-based evaluation criterion of geometric deviation

As earlier mentioned the traditional evaluation criterion for variation simulation is the deviation and variation in each node of the assembly. The stiffness of the parts is of course affecting the deviation of the subassembly. However, in many cases the deviation is not as important as how the subassembly behaves in the next assembly step. As an example, a really flexible subassembly will, when assembled to a stiffer subassembly, form according to the mating subassembly. Therefore, its deviation is less likely to propagate to downstream assembly stations [23]. A complementary evaluation criterion reflecting this behavior is to investigate how much work or energy that is required for the next assembly step. The strain energy is the energy stored in an isotropic, ductile part as a result of an elastic deformation of the part, i.e. in this context, the work done to assemble the evaluated subassembly in the next assembly step. The strain energy can be divided into strain energy due to volume changes of the part (sometimes referred to as hydrostatic stresses) and strain energy due to distortion of the part (sometimes referred to as deviatoric stresses) [24]. For a subassembly discretized into a finite element mesh, the strain energy per unit volume can be considered and is then called the strain energy density, **W** [25]. Using the notation from Section 2, the strain energy density can be derived and expressed as

$$\mathbf{W} = \frac{1}{2} \mathbf{u}^T \mathbf{K} \, \mathbf{u} \tag{5}$$

For this derivation, the reader is referred to for example [25]. The strain energy density **W** is a *p*x1 vector, where *p* is the number of nodes in the mesh representation of the subassembly. Summarizing over the elements in the vector will give the total work or energy required to assemble a part or a subassembly to another part or subassembly:

$$W_{tot} = \mathbf{1}^T \mathbf{W} \tag{6}$$

3.1. Case study, part

The suggested method is mainly aimed at serving as an evaluation criterion for subassemblies, complementing geometric deviation and/or variation which are the standard criteria. However, the method can also be applied on part level. Here, a very simple example, see Fig. 1, is used. This can also serve as a validation of the calculation procedure, since it can be compared to an analytical solution.
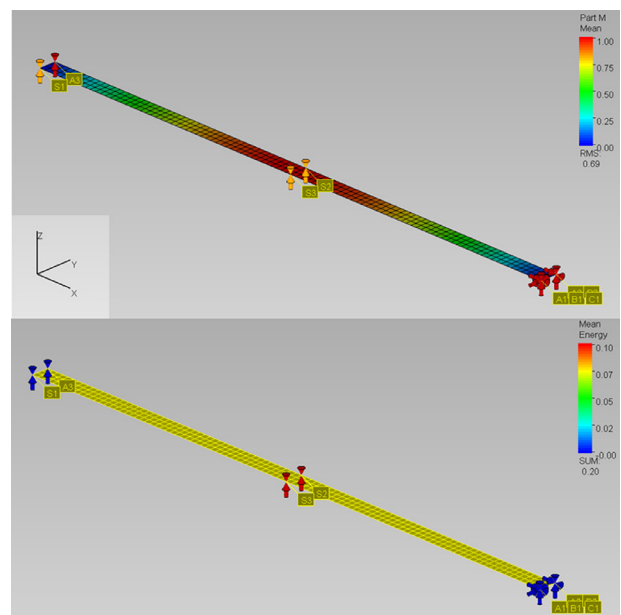
Fig. 1. Upper: The bean is deviating 1 mm in Z-direction in the middle of the beam. Lower: The energy W_{tot} required to clamp it to nominal equals 0.20 Nmm (0.1 Nmm in each one of the two clamps in the middle, as shown by the color-coding of the arrows).

The analytical solution can easily be found by utilizing the basic formula for three point bending with a central load [26], i.e.

$$\delta = \frac{F * l^3}{48E * (w * t^3 / 12)},\tag{7}$$

where δ is the deformation, F is the applied central force, l is the length of the beam, E is Young's modulus, w is the beam width and t is the beam thickness. Solving the equation for F and utilizing that the applied work can be calculated as $0.5 * F * \delta$ gives 0.20 Nmm, which agrees well with W_{tot} in Fig. 1.

3.2. Case study, subassembly

The evaluation criterion suggested above will be applied to a case study from the automotive industry, see Fig. 2. The color-coding shows part deviations based on scan data. The parts will be joined using spot welding to form the subassembly in Fig. 3, denoted "Subassy1". The color-coding in Fig. 3 shows the predicted assembly deviation based on the simulation methodology outlined in Section 2. The simulation is done in the software RD&T [27].

In the next assembly step "Subassy1" is supposed to be joined to the three gray parts shown in Fig. 4 to form "Subassy2". The focus here is to evaluate the energy required to form "Subassy2" and use
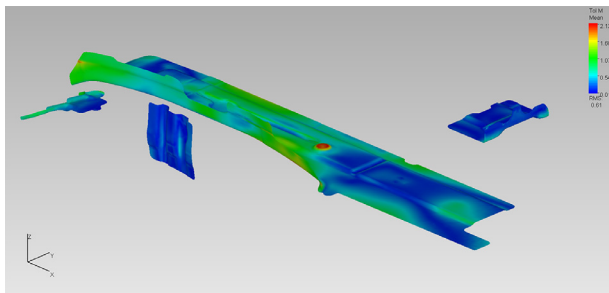
that to evaluate the quality of "Subassy1". For simplicity, the gray parts in "Subassy2" are supposed to be nominal.

In Fig. 5, the energy-based evaluation criterion from Eq (4) is calculated and the values in each node where energy is applied is color-coded. This covers clamps, joining points and nodes affected by contact forces. Also the sum over all nodes are calculated (as shown in Eq. (5)). The value of W_{tot} is 786 Nmm. In this case, the parts constituting "Subassy1" were supposed to have Young's modulus E = 210 GPa, which is the standard value for sheet metal.

As an alternative to this, the stiffness of the parts constituting "Subassy1", was lowered to E = 2 GPa, corresponding to ABS plastic. Again, the energy required to assemble "Subassy1" to some nominal parts to form "Subassy2" was calculated. The results can be seen in Fig. 6 and the value of Wtot is now 7 Nmm, i.e. much lower than for the more rigid subassembly.

Fig. 2. The four parts that will form a subassembly ("Subassy1"). The color-coding shows part deviations based on scan data.
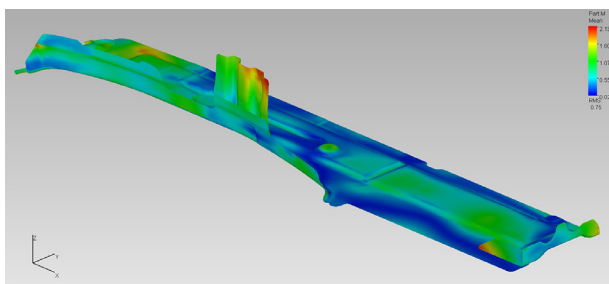

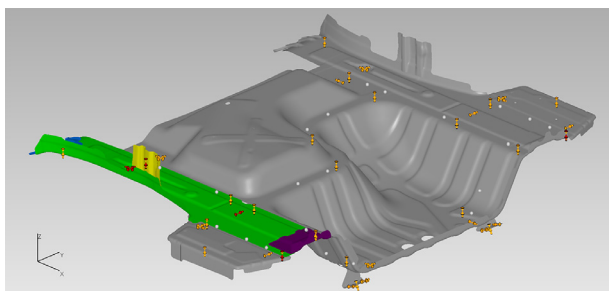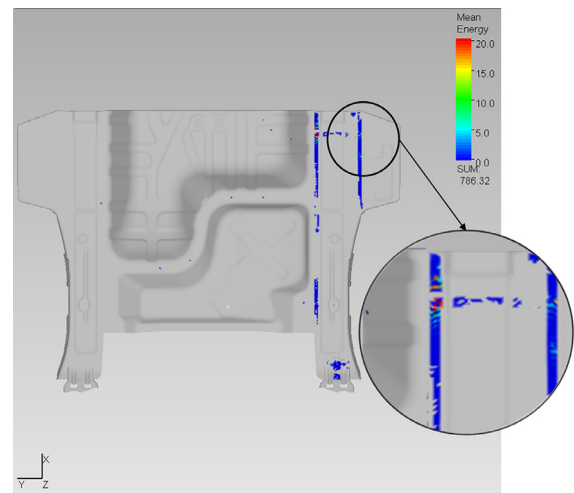**Fig. 3.** Color-coding of the simulated deviation of "Subassy1".

Fig. 4. "Subassy 1″ from Fig. 3 will be assembled to other parts to form "Subassy2" shown in this picture. The arrows show clamps/locators and the gray spheres welding points.

Fig. 5. The required energy to assembly Subassy1 to other parts to form Subassy2. The stiffness of all parts are 210 GPa.
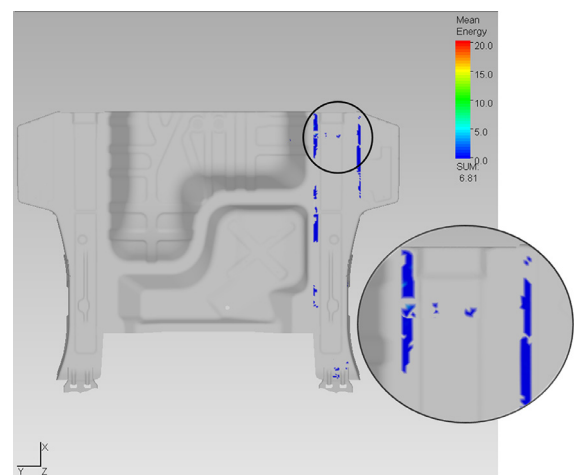

Fig. 6. The required energy to assembly Subassy1 to other parts to form Subassy2. The stiffness of all parts are 2 GPa.

The point here is that both the versions of "Subassy1" will get the same result when evaluated in the traditional way using RMS values or a color-coding of the deviation of the assembly, as shown in Fig. 3. The change in stiffness (i.e. material) will not affect the result, due to the fact that all the parts in the subassembly are supposed to have the same Young's modulus and then it will cancel out in the calculations. Therefore, the complementary evaluation criterion based on energy required to assemble the subassembly to other parts in the next assembly step is suggested.

4. Discussion

In the case studies, sheet metal parts have been replaced with plastic parts. This is not a realistic scenario, but its purpose was to illustrate how the stiffness of a part or subassembly affects its behavior in subsequent assembly steps. It should also again be noted that if all the parts in a subassembly have the same Young's modulus, the resulting deviation of that subassembly will not depend on the material, i.e. a subassembly of plastic parts or sheet metal parts will have the same deviation but the work required in the next assembly step will differ.

In this work, a static analysis of the strain energy has been conducted. This means that the deviation, u, after, and not during, joining of the parts in an assembly is considered. During the joining process the deviation, and the strain energy, may vary. As an example, if several spot welds are set in a sequence, the strain energy after a few executed spot welds might differ from the strain energy in the complete assembly after completing all spot welds. However, the strain energy-based criterion is supposed to complement the simulated final assembly geometric deviation and variation and can therefore be calculated based on the final assembly deviation. A limitation of this work is that only non-linearity due to contacts between parts is included. In [28], also the effects of material and geometric non-linearity are discussed and in [29], the inclusion of plastic strain in variation simulation is explored. Non-linearity in the material can be interesting to include in future work, especially for highly flexible parts where large deformations leading to non-linear behavior can be expected.

For future work, it will also be interesting to investigate how mixed materials affect the energy-based criterion and how the stiffness of parts can be included in the choice of locating schemes.

5. Summary and conclusion

In the paper, the stiffness was varied for a case study. Given that each one of the parts has the same geometrical deviation for both stiffnesses, the more flexible parts will transmit less of their deviation when assembled to another part or subassembly in a downstream assembly step. It was shown that the energy-based criterion suggested in this paper displayed this difference, while the traditional criterion based on the geometric deviation did not. The geometric deviation and variation on the assembly level should still be the major evaluation criteria, but when studying non-rigid parts, the authors believe the suggested criterion based on the work required to join the part or subassembly to its mating parts in the next assembly step can add valuable information concerning the severity of the deviation and variation. The main purpose and conclusion of this paper were to show this phenomenon and suggest an evaluation criterion taking this into account.

Other conclusions that can be drawn are that the since the suggested energy-based criterion can be calculated based on the deviation and the stiffness matrix, it can be easily calculated without adding much simulation time, and that color coding can be used to identify areas with high-strain energy.

Declaration of Competing Interest

The authors declare that they have no known competing financial interests or personal relationships that could have appeared to influence the work reported in this paper.

References

[1] Morse E, Dantan J-Y, Anwer N, Söderberg R, Moroni G, Qureshi A, Jiang X, Mathieu L (2018) Tolerancing: managing uncertainty from conceptual design to final product. *CIRP Ann.* 67(2):695–717.

[2] Wang Y, Li L, Hartman NW, Sutherland JW (2019) Allocation of assembly tolerances to minimize costs. *CIRP Ann.* 68(1):13–16.

[3] Tsutsumi D, Gyulai D, Kovács A, Tipary B, Ueno Y, Nonaka Y, Monostori L (2018) Towards joint optimization of product design, process planning and production planning in multi-product assembly. *CIRP Ann.* 67(1):441–446.

[4] Söderberg R, Lindkvist L, Wärmefjord K, Carlson JS (2016) Virtual geometry assurance process and toolbox. *Procedia CIRP* 43:3–12.

[5] Polini W (2012) Taxonomy of models for tolerance analysis in assembling. *Int. J. Prod. Res.* 50(7):2014–2029.

[6] Roucoules L, Anwer N (2021) Coevolution of digitalisation, organisations and product development Cycle. *CIRP Ann.* 70(2):519–542.

[7] Söderberg R, Wärmefjord K, Lindkvist L (2015) Variation simulation of stress during assembly of composite parts. *CIRP Ann.* 64(1):17–20.

[8] Wärmefjord K, Söderberg R, Lindkvist L (2013) Simulation of the effect of geometrical variation on assembly and holding forces. *Int. J. Product. Develop.* 18(1):88.

[9] Vasiliev A, Lupuleac S, Shinder J (2021) Numerical approach for detecting the resonance effects of drilling during assembly of aircraft structures. *Mathematics* 9 (22):2926.

[10] Yang J, Xiong J, McBean I, Havakechian S, Liu F, Luo J (2017) Performance impact of manufacturing variations for multistage steam turbines. *J. Propul. Power* 33 (4):1031–1036.

[11] Fang Y, Jin X, Huang C, Zhang Z (2017) Entropy-based method for evaluating contact strain-energy distribution for assembly accuracy prediction. *Entropy* 19(2):49.

[12] ISO Standard. ISO 1101-2017 geometrical product specifications (GPS)—geometrical tolerancing—tolerances of form, orientation, location and run-out. *Switzerland: ISO, 1101*, 2017.

[13] ASME. *ASME Y14.5-2018: Dimensioning and Tolerancing*, American Society of Mechanical EngineersNY.

[14] Morse E, Grohol C (2019) Practical conformance evaluation in the measurement of flexible parts. *CIRP Ann.* 68(1):507–510.

[15] Lindau B, Wärmefjord K, Lindkvist L, Söderberg R (2020) Virtual fixturing: inspection of a non-rigid detail resting on 3-points to estimate free state and overconstrained shapes. In: *Proc. ASME 2020 International Mechanical Engineering Congress and Exposition V02BT02A065*,

[16] Abenhaim GN, Desrochers A, Tahan AS, Bigeon J (2015) A virtual fixture using a FE-based transformation model embedded into a constrained optimization for the dimensional inspection of nonrigid parts. *Comput. Aided Des.* 62:248–258.

[17] Liu SC, Hu SJ (1997) Variation simulation for deformable sheet metal assemblies using finite element methods. *J. Manuf. Sci. Eng.* 119:368–374.

[18] Wärmefjord K, Söderberg R, Lindau B, Lindkvist L, Lorin S (2016) Joining in non-rigid variation simulation. *Computer-aided Technologies-Applications in Engineering and Medicine*, IntechOpen.

[19] Wärmefjord K, Söderberg R, Lindkvist L (2008) Tolerance simulation of compliant sheet metal assemblies using automatic node-based contact detection. In: *Proc. Proceedings of ASME IMECE 2008*, .

[20] Lindau B, Lorin S, Lindkvist L, Söderberg R (2016) Efficient contact modeling in nonrigid variation simulation. *J. Comput. Inf. Sci. Eng.* 16(1):011002. -011002.

[21] Stefanova M, Minevich O, Baklanov S, Petukhova M, Lupuleac S, Grigor'ev B, Kokkolaras M (2020) Convex optimization techniques in compliant assembly simulation. *Optimiz. Eng.* 21(4):1665–1690.

[22] Tabar RS, Lorin S, Cromvik C, Lindkvist L, Wärmefjord K, Soderberg R (2021) Efficient spot welding sequence simulation in compliant variation simulation. *J. Manuf. Sci. Eng.* : 1–12.

[23] Hu SJ (1997) Stream-of-variation theory for automotive body assembly. *CIRP Ann.* 46(1):1–6.

[24] Hern E (1997) *Mechanics of Materials 1 - An Introduction to the Mechanics of Elastic and Plastic Deformation of Solids and Structural Materials*, Elsevier: Amsterdam.

[25] Bower AF (2009) *Applied Mechanics of Solids*, CRC press.

[26] Gere JM, Goodno BJ (2012) *Mechanics of Materials*, Cengage learning.

[27] RD&T Technology, 2022, "RD&T webpage," http://rdnt.se/.

[28] Liu T, Li Z-M, Jin S, Chen W (2019) Compliant assembly analysis including initial deviations and geometric nonlinearity—part I: beam structure. *Proc. Inst. Mech. Eng. Part C J. Mech. Eng. Sci.* 233(12):4233–4246.

[29] Camuz S, Lorin S, Wärmefjord K, Söderberg R (2019) Nonlinear material model in part variation simulations of sheet metals. *J. Comput. Inf. Sci. Eng.* 19(2).